Mechanochemical synthesis and characterization of nanodimensional iron–cobalt spinel oxides

E. Manova[a,*], D. Paneva[a], B. Kunev[a], Cl. Estournès[b], E. Rivière[c], K. Tenchev[a], A. Léaustic[c], I. Mitov[a]

[a] *Institute of Catalysis, Bulgarian Academy of Sciences, Acad. G. Bonchev St., Block 11, 1113 Sofia, Bulgaria*
[b] *CNRS - Institut Carnot, CF - 31062 Toulouse, France*
[c] *Institut de Chimie Moléculaire et des Matériaux d'Orsay, UMR8182, Equipe Chimie Inorganique, Université Paris-Sud XI, 91405 Orsay, France*

A B S T R A C T

Iron–cobalt spinel oxide nanoparticles, $Co_xFe_{3-x}O_4$ ($x = 1, 2$), of sizes below 10 nm have been prepared by combining chemical precipitation with high-energy ball milling. For comparison, their analogues obtained by thermal synthesis have also been studied. The phase composition and structural properties of the obtained materials have been investigated by means of X-ray diffraction, Mössbauer spectroscopy, infrared spectroscopy, temperature-programmed reduction and magnetization measurements. X-ray diffraction shows that after 1 h of mechanical treatment ferrites are formed. The measurement techniques employed indicate that longer milling induces an increase in crystal size while crystal defects decrease with treatment time. Magnetization and reduction properties are affected by the particles size, the iron/cobalt ratio and the synthesis conditions.

Keywords:
Nanostructured materials
Cobalt ferrite
Mechanochemical processing
Magnetization
Mössbauer spectroscopy

1. Introduction

Nowadays the synthesis of spinel ferrite nanoparticles has been intensively studied, because of their remarkable electrical and magnetic properties and wide practical application to information storage system, ferrofluid technology, magnetocaloric refrigeration, catalysis, and medical diagnostics. The principal role of the preparation conditions on the morphological and structural features of the ferrites have been discussed in several papers [1–6]. High-energy milling as a solid-state method of synthesis of nanodimensional materials has been the subject of considerable interest in recent years [7–10]. The highly non-equilibrium nature of the milling process creates the opportunities to prepare solids of improved and/or novel physical and chemical properties. Mechanical milling is a technique with an advantage that it can easily be operated and produces large amounts of nanostructured powders for a short period of time [11]. A mechanochemical route for the preparation of ferrites has been reported [12–15], however, synthesis was generally performed starting from a mixture of iron and other metal oxides. In our previous studies, we reported ferrites formation after a mechanical milling of the corresponding hydroxide carbonates [16,17]. Among spinel ferrites, cobalt ferrite $CoFe_2O_4$ is especially interesting because of the high cubic magnetocrystalline anisotropy, high coercivity, and moderate saturation magnetization. The properties of these ferrites are highly sensitive to the concentration of divalent metal ions, to substituting other metallic ions for the divalent ions and to the crystallite size [18–21]. Many synthesis strategies for preparing nanosized cobalt ferrite have been reported [21–25].

In this paper, for the first time we describe the mechanochemical synthesis of Co_2FeO_4. We also present the mechanochemical synthesis of $CoFe_2O_4$ under the same conditions as for Co_2FeO_4 and the characterization of the obtained materials using powder X-ray diffraction, Mössbauer spectroscopy, infrared spectroscopy, temperature-programmed reduction, and magnetic measurements of samples prepared at different milling times.

2. Experimental

The synthesis was performed by two steps: co-precipitation and mechanical milling of the co-precipitation precursors. The starting materials used were $Fe(NO_3)_3{\cdot}9H_2O$ powder (purity 99%), $Co(NO_3)_2{\cdot}6H_2O$ powder (purity 96%), and Na_2CO_3. In the co-precipitation processing route, a 0.5 M solution of metal salts containing Co and Fe were taken in a desired molar ratio: Fe/Co = 2 and 0.5. Mixtures of cobalt and iron hydroxide carbonates precursors were formed when a 1 M sodium carbonate solution was added at pH 9. The precipitates were washed and dried at 348 K for 3 h. The as-obtained precursors (named as CoFe2HC and Co2FeHC) were milled using a Fritsch Planetary mill in a hardened steel vial together with 15 grinding balls having different diameters (from 3 to 10 mm). The ball-to-powder mass charge ratio was 10:1. The powders were milled for 1 and 3 h (samples denoted as CoFe2MS1, CoFe2MS3, Co2FeMS1, and Co2FeMS3, where MS indicates mechanochemical synthesis). Thermal synthesis was performed in two steps: co-precipitation (starting materials and procedure are described above) and subsequent annealing of the co-precipitation precursor at 773 and 573 K for $CoFe_2O_4$ (denoted as CoFe2TS, where

Corresponding author. Tel.: +359 2 979 2528; fax: +359 2 971 2967.
E-mail addresses: elina@ic.bas.bg, elbg2001@yahoo.com (E. Manova).

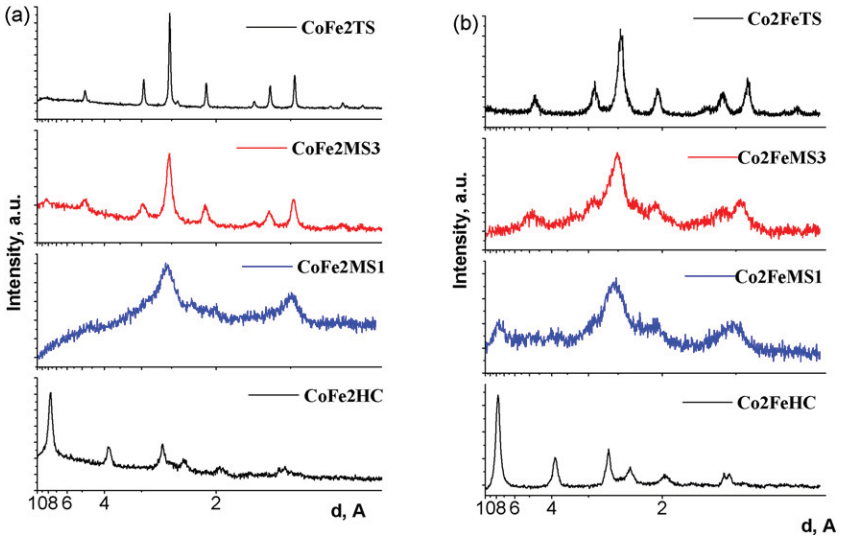

Fig. 1. Powder X-ray diffraction patterns of $CoFe_2O_4$ (a) and Co_2FeO_4 (b) precursors after different milling times and thermal treatment.

TS indicates thermal synthesis) and Co_2FeO_4 (denoted as Co2FeTS), respectively. According to our previous results [26] the thermal treatment of Co2Fe-hydroxide carbonate at temperatures above 573 K leads to the formation of two spinels of different Co/Fe ratio, while for $CoFe_2O_4$ this temperature is too low for spinel formation and for this reason the CoFe2-hydroxide carbonate is annealed at 773 K.

The structure was determined by X-ray diffraction (XRD) using TUR M62 diffractometer with Co Kα radiation. Data analysis was carried out using JCPDS database. Transmission Mössbauer spectra were obtained at room temperature (RT) with a Wissel electromechanical Mössbauer spectrometer (Wissenschaftliche Elektronik GmbH, Germany) working at a constant acceleration mode. A ^{57}Co/Cr (activity ≅ 10 mCi) source and an α-Fe standard were used. Experimentally obtained spectra were treated using the least squares method. The parameters of hyperfine interaction such as isomer shift (IS), quadrupole splitting (QS), and effective internal magnetic field (H_{eff}) as well as line widths (FWHM) and relative spectral area (G) of the partial components of the spectra were determined. The infrared (IR) spectra were taken on a Spectrum 1000 (PerkinElmer) FTIR spectrometer in KBr pellets. Isothermal magnetizations at RT were obtained with a Princeton Applied Research vibrating sample magnetometer Model 155 (VSM – maximum static field of ±1.8 T). Temperature and field dependences of the magnetization of the cobalt ferrites were measured on a Quantum Design SQUID Magnetometer. Zero-field cooled (ZFC) magnetization of the sample was measured by cooling down the sample to 5 K in zero-field and monitoring the magnetization of the sample from 5 to 400 K in a field of 20 Oe. The field-cooled (FC) magnetization was measured by cooling the sample down to 5 K in the same field. In order to avoid sample rotation in the applied field the nanoparticles were embedded in a polymer matrix, PMMA (poly methyl methacrylate). Transmission electron microscopy (TEM) investigations were made using a Topcon 002B electron microscope operating at 200 kV with a point-to-point resolution r = 1.8 Å. The samples were sonicated in ethanol and deposited on the copper grid precovered by polymer. Temperature-programmed reduction (TPR) of the samples was carried out in the measurement cell of a differential scanning calorimeter (DSC-111, SETARAM) directly connected to a gas chromatograph (GC). Measurements were carried out in the 300–973 K range at a 10 K/min heating rate in flow of Ar:H_2 = 9:1, the total flow rate being 20 ml/min. A cooling trap between DSC and GC removes the water obtained during the reduction.

3. Results and discussion

XRD patterns of the precursors and those of the samples obtained after different milling times as well as after thermal treatment are shown in Fig. 1. The patterns of the precursors are characteristic of layered double hydroxides (LDH) as found for pyroaurite (PDF 25-0521) and hydrotalcite (PDF 41-1428). After 1 h of milling the intensive lines of LDH disappeared and broad peaks of a new phase were registered. Their positions and intensities suggest the formation of a spinel phase with cubic structure. After 3 h of milling, the diffraction lines of the spinel phase ($CoFe_2O_4$ or Co_2FeO_4) are well defined. The average crystallites size (D), the degree of microstrain (e) and the lattice parameter (a) of the studied cobalt ferrites were determined from the experimental XRD profiles (Table 1) by using the Williamson–Hall equation [27]:

$$\beta cos\,\theta = \frac{0.9\lambda}{D} + 4\varepsilon \sin\theta \quad (1)$$

where β is the full width at half maximum (FWHM) of the XRD peaks, θ is the Bragg angle, λ is the X-ray wavelength, D is the crystallite size, and ε is the value of internal strain. By plotting the value of $\beta\cos\theta$ as a function of $4\sin\theta$ the microstrain ε may be estimated from the slope of the curve, whereas the crystallite size D can be obtained from the intersection with the vertical axis. A well-defined effect of the crystal size increase and decrease in the crystal defects and lattice parameter with milling time is observed with the mechanochemically prepared materials.

Typical morphologies of the synthesized $Co_xFe_{3-x}O_4$ (x = 1, 2) particles visualized by TEM show that in all cases the prepared particles are nanosized, nearly spherical in shape and tend to agglomerate. As an example transmission electron micrographs of Co2FeTS and CoFe2MS3 are presented in Fig. 2. The average values of particles diameter estimated from the TEM images are in good agreement with those calculated from XRD results.

The bands characteristic of carbonate groups vibrations (1480, 1345, 1100, 840 cm^{-1}) and those due to M–O stretching mode (350 cm^{-1}) and M–OH vibrations (475, 710 cm^{-1}) appear in the IR spectra (not shown) of the hydroxide carbonate precursors. In the IR spectra of the samples obtained after 1 h of mechanical treatment the bands of the carbonate vibrations are less intense and two bands characteristic of spinel phases appear. The IR spectra of samples mechanically treated for 3 h and the thermally obtained samples present only bands typical of a spinel phase (Fig. 3). The higher frequency band ν_1 is due to AOB_3, and that of the lower frequency (ν_2) arises from the BOB_2 vibrations in the spinel lattice, where A and B denote cations in tetrahedral and octahedral sites, respectively, of the spinel structure [28]. For Co_2FeO_4 the

Table 1
Crystallite size (D), microstrain (e) and lattice parameter (a) of investigated samples.

Sample	D (nm)	$e \times 10^3$ (a.u.)	a (Å)
CoFe2MS1	3.4	8.97	8.42
CoFe2MS3	8.6	7.83	8.40
CoFe2TS	18.9	1.80	8.37
Co2FeMS1	2.7	11.50	8.39
Co2FeMS3	3.8	8.08	8.29
Co2FeTS	10.5	7.20	8.26

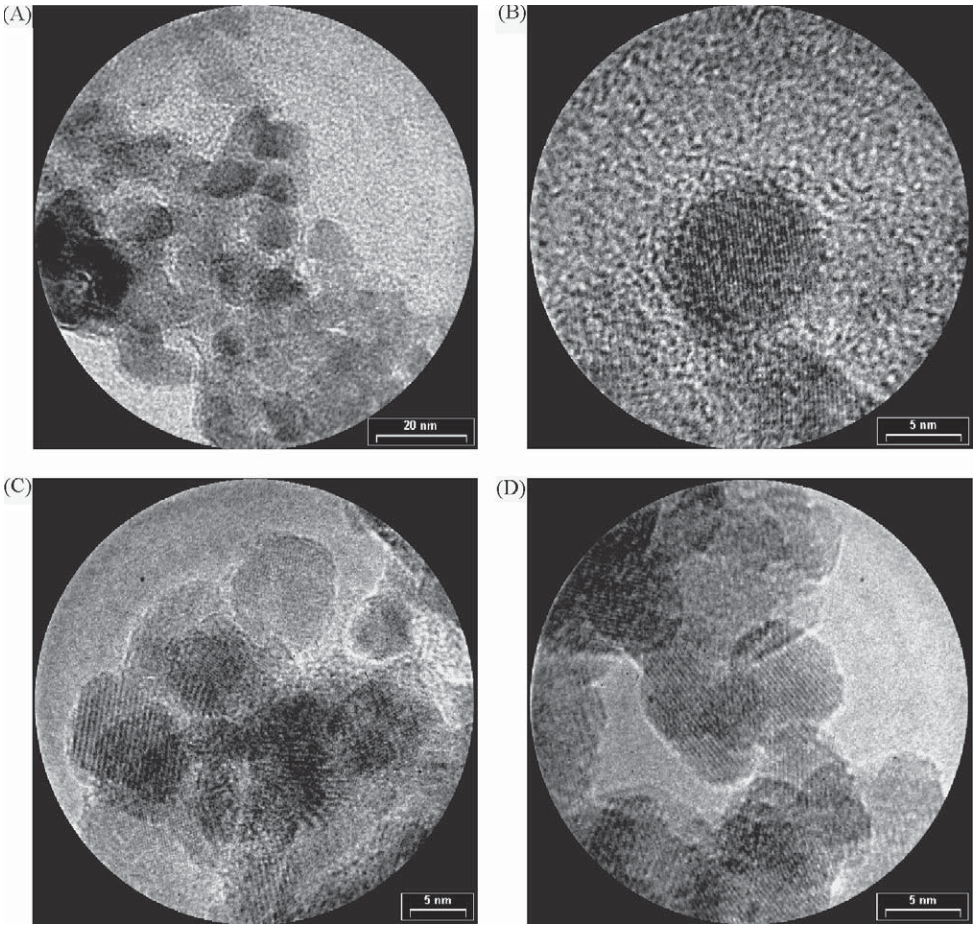

Fig. 2. Transmission electron micrograph of Co2FeTS (A–C) and CoFe2MS3 (D).

ν_1 and ν_2 positions in the transmission spectra are almost the same ($\nu_1 \approx 650\,cm^{-1}$, $\nu_2 \approx 560\,cm^{-1}$) independent of the preparation method. For all the $CoFe_2O_4$ samples, the ν_1 and ν_2 positions are around 590 and 385 cm^{-1}, respectively, with a small shift to higher wavenumbers for the mechanochemically obtained sample. This change in band position may be due to a change of the internuclear distance of M–O in the equivalent lattice sites. The observed vibration bands are in agreement with the results obtained by Waldron [29], Silva et al. [30], and Lefez et al. [31]. It can be seen that for iron rich spinels the main bands are shifted to lower frequencies, indicating weaker force constants for Fe–O bonds compared to Co–O. The bands of the thermally obtained samples narrowed due to the increase of crystallization.

TPR profiles of mechanochemically and thermally obtained materials are presented in Fig. 4 and show mainly one reduction peak with shape and maximum position depending on the iron/cobalt ratio. A broadening is observed for the iron-rich samples and a shift of the peak maxima towards higher temperatures compared to the cobalt-rich ones. For the studied iron–cobalt mixed oxides the elementary steps of Fe^{3+}, Co^{3+}, and Co^{2+} reduction cannot be distinguished from the TPR curves, thus leading to the suggestion that the more easily reducible cations (in this case Co^{3+} and Co^{2+}) promote the reduction of iron cations. CoFe2MS3 is reduced in the range of 400–750 K with peak maximum at 650 K and a shoulder at ca. 700 K. It is clearly seen that these two reduction peaks are shifted to a higher temperature with the thermally pre-

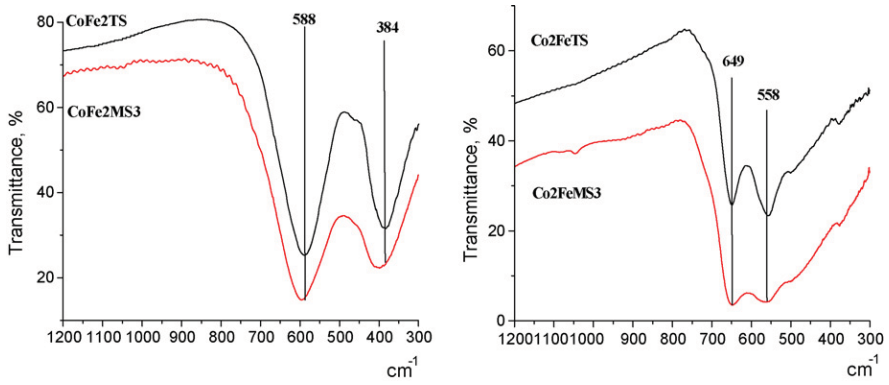

Fig. 3. IR spectra of mechanochemically and thermally obtained cobalt ferrites.

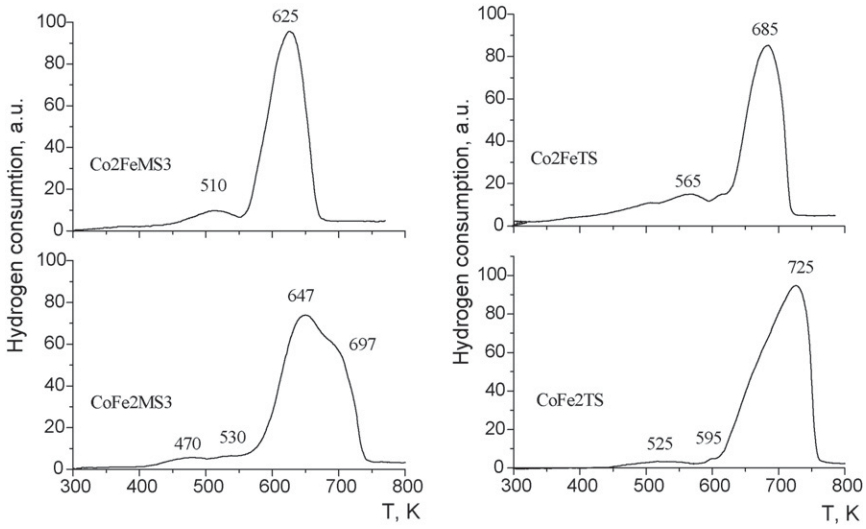

Fig. 4. TPR of mechanochemically and thermally obtained cobalt ferrites.

pared sample. This more difficult reduction can be due to increased crystallinity of the sample obtained by thermal treatment in comparison with the mechanochemically synthesised one. In the case of Co_2FeO_4, mainly one reduction peak is observed that can be due to a larger amount of cobalt present in the samples. As for $CoFe_2O_4$, the peak of the thermally synthesised sample is shifted to higher temperatures and the reason is probably a higher crystallinity.

Mössbauer spectroscopy was applied to gain information about the cationic occupations and/or different state distribution of iron ions in the studied ferrite materials. Fig. 5 shows RT Mössbauer spectra of samples taken from different steps of the processing route. The corresponding parameters determined from simulations of the spectra are listed in Table 2. The co-precipitated precursors exhibit a quadrupole doublet with IS = 0.34 mm/s, QS = 0.65–0.70 mm/s, indicating that the hydroxide carbonates are paramagnetic. As shown in Fig. 5b the spectra of Co_2FeO_4 appear always as doublets. The spectra of CoFe2MS1 and CoFe2MS3 are doublets, while the spectrum of CoFe2TS contains only sextet components (Fig. 5a). It should be noted that reasonable data fitting of the Mössbauer spectrum of CoFe2TS exhibiting magnetic splitting at RT could be obtained only when the B-site pattern is assumed to be a superposition of more than one sextet. In our case the hyperfine interaction of the B site could be fitted up to the four overlapping six-line pattern (belonging to high spin Fe^{3+} ions with 0–3 Co nearest neighbours), which is in agreement with observations of other authors for ferrite samples [12,32]. The experimentally calculated intensity ratio of the B-site peaks is different from that calculated using a binomial distribution, proposed by Sawatzky et al. [33] and de Bakker et al. [34]. The reason for the observed difference is the method of preparation, which does not ensure a statistical equilibrium distribution of the metal ions in the ferrite sample. Additionally the size effect of small particles could increase the relative spectral area of the components having smaller H_{eff}. The results obtained after simulation of the Mössbauer spectrum indicate that the spinel structure of the thermally obtained compound is not completely inverse (of the order of 10% Co on A sites).

Taking into account the XRD data we suppose that the doublets observed in all milled samples and Co2FeTS arise from Fe(III) ions in ultrafine ferrite particles exhibiting superparamagnetic behaviour [35]. To confirm the superparamagnetic behaviour magnetic measurements were carried out.

Room temperature isothermal magnetizations of the mechanochemically and thermally prepared phases are shown in Figs. 6 and 7, respectively. The magnetizations of all samples obtained after mechanochemical treatment are weak (a few emu/g). The small value of the measured magnetization could be related to strong magnetic anisotropy and possible local canting of magnetic ions due to the imperfect structure, and mainly to the surface effect of nanosize particles of large surface area. The absence of saturation in the magnetic field range explored, the "S" shape of the curves together with the lack of coercivity indicate the presence of small magnetic particles exhibiting superparamagnetic behaviour [36]. This particle size effect is in good agreement with the room temperature Mössbauer spectrometry where only doublet components are observed. The RT magnetization of CoFe2TS is 63.2 emu/g and the coercive field – 1.5 kOe. Cobalt ferrite bulk material ($CoFe_2O_4$) is known to be a ferrimagnetic material with very high cubic magnetocrystalline anisotropy

Table 2
Mössbauer parameters of samples after different milling times.

Sample	Compounds	IS (mm/s)	QS (mm/s)	H_{eff} (T)	FWHM (mm/s)	G (%)
CoFe2MS1	Fe^{3+}, $CoFe_2O_4$	0.34	0.67	–	0.48	100
CoFe2MS3	Fe^{3+}, $CoFe_2O_4$	0.34	0.65	–	0.57	100
CoFe2TS	Sx 1 – Fe^{3+}, $CoFe_2O_4$	0.28	0.00	49.0	0.41	44
	Sx 2 – Fe^{3+}, $CoFe_2O_4$	0.37	0.00	52.4	0.42	18
	Sx 3 – Fe^{3+}, $CoFe_2O_4$	0.37	0.00	50.7	0.42	16
	Sx 4 – Fe^{3+}, $CoFe_2O_4$	0.37	0.00	46.7	0.42	15
	Sx 5 – Fe^{3+}, $CoFe_2O_4$	0.37	0.00	43.2	0.42	8
Co2FeMS1	Fe^{3+}, Co_2FeO_4	0.34	0.70	–	0.49	100
Co2FeMS3	Fe^{3+}, Co_2FeO_4	0.33	0.66	–	0.47	100
Co2FeTS	Fe^{3+}, Co_2FeO_4	0.32	0.73	–	0.47	100

IS: isomer shift relative to metallic α-Fe at RT; QS: quadrupole splitting for doublets or quadrupole shift for sextets; H_{eff}: effective magnetic field.

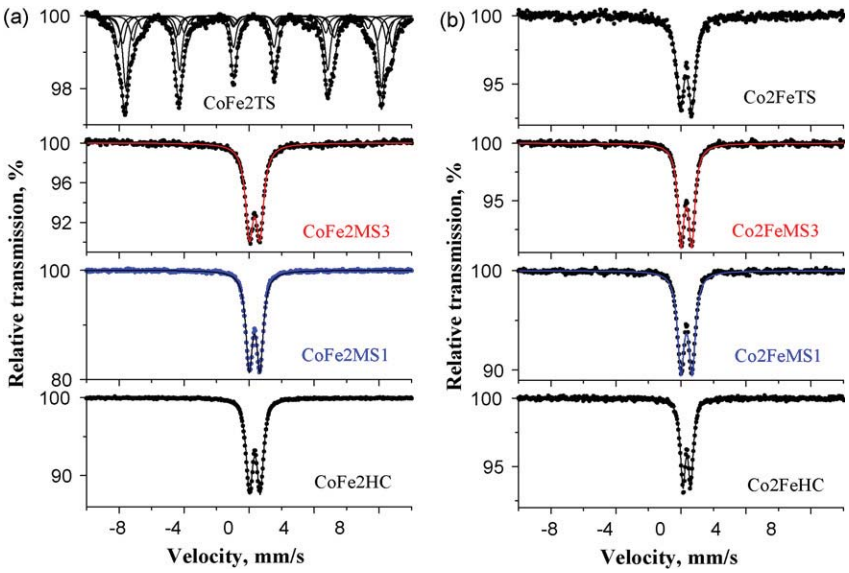

Fig. 5. Mössbauer spectra of $CoFe_2O_4$ (a) and Co_2FeO_4 (b) precursors after different milling times.

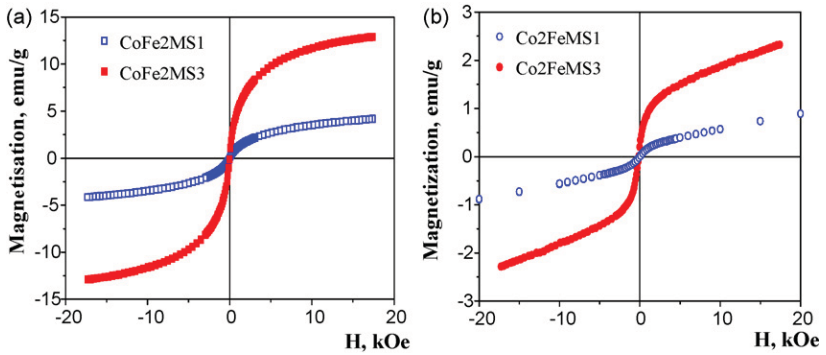

Fig. 6. Isothermal magnetizations of $CoFe_2O_4$ (a) and Co_2FeO_4 (b) after different milling times.

leading to high theoretical coercivity: 25.2 and 5.4 kOe at 5 and 300 K, respectively, and a saturation magnetization of 93.9 and 80.8 emu/g at 5 and 300 K, accordingly [37,38]. However, the values of the magnetic properties of CoFe2TS are lower than the values of pure crystalline cobalt ferrite indicating that either the objects formed are core/shell particles with spin-glass-like surface layer [39] or that some of the ultrafine particles with superparamagnetic behaviour remain intact. Our values are in accordance with results obtained with nanocrystalline $CoFe_2O_4$ of similar grain size [40]. Concerning Co_2FeO_4, it is important to note that saturation of the magnetization is never reached (in the magnetic field range used (5 T)). The absence of coercivity, remanence, and saturation at 295 K (Figs. 6b and 7b) can be explained by size effects and suggests that this material behaves as a superparamagnetic at room temperature.

Magnetization measurements as a function of applied temperature have been performed and as an example, the FC-ZFC curves of CoFe2MS3 and Co2FeMS1 are presented in Fig. 8. The blocking temperature (TB) associated with the maximum in the zero field cooling magnetization curve increases with the milling time and the iron content (170 and 210 K for CoFe2MS1 and CoFe2MS3; 75 and 110 K for Co2FeMS1 and Co2FeMS3, respectively). TB can be associated with an average size of the particles. The increase of the particle size is confirmed by the increase of the blocking temperature with

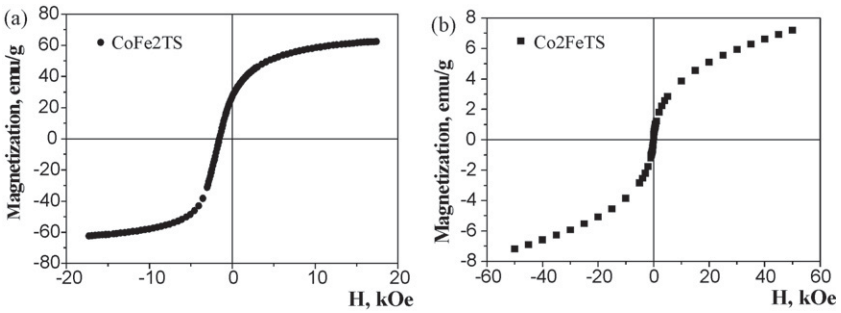

Fig. 7. Isothermal magnetizations of thermally synthesized $CoFe_2O_4$ (a) and Co_2FeO_4 (b).

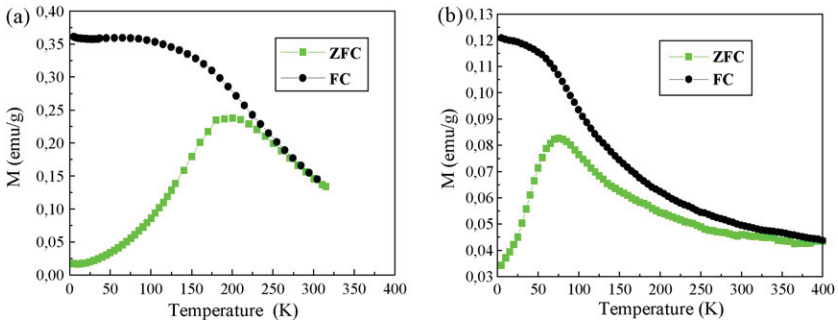

Fig. 8. ZFC-FC measurements of CoFe2MS3 (a) and Co2FeMS1 (b).

mechanochemical treatment time and is in accordance with the XRD, TEM, and Mössbauer spectroscopy results. The point at which ZFC-FC starts to diverge is usually associated with the blocking temperature of the larger particles. The difference between these two temperatures reflects the distribution in the particle size. Thus, the cobalt rich sample exhibits a wide particles size distribution with the larger particles magnetically blocked at room temperature.

4. Conclusions

High-energy ball milling of layered cobalt–iron hydroxide carbonates results in the formation of nanocrystalline cobalt ferrites, where the particle size is below 10 nm and can be controlled by the treatment time. The measurement techniques employed indicate that the crystal size increases while the number of defects decreases with treatment time. The magnetic and reduction properties of the obtained materials are affected by the synthesis conditions, the iron/cobalt ratio, and the particles size. This work shows that nanosized $CoFe_2O_4$ and Co_2FeO_4 particles can be synthesized by combining the co-precipitation method with subsequent high-energy ball milling. This is a promising technique for a relatively large-scale preparation of cobalt ferrite nanoparticles with tailored properties.

Acknowledgements

The authors thank the National Science Fund of Bulgaria for financial support through Projects X-1504/05 and Rila4-412 (DO 02-29/2008).

References

[1] K.V.P.M. Shafi, A. Gedanken, R. Prozorov, J. Balogh, Chem. Mater. 10 (1998) 3445–3450.
[2] Y. Köseoğlu, A. Baykal, M.S. Toprak, F. Gözuak, A.C. Başaran, B. Aktaş, J. Alloys Compd. 462 (2008) 209–213.
[3] B.G. Toksha, S.E. Shirsath, S.M. Patange, K.M. Jadhav, Solid State Commun. 147 (2008) 479–483.
[4] B. Baruwati, S.V. Manorama, Mater. Chem. Phys. 112 (2008) 631–636.
[5] S. Lee, V.T. John, C. O'Connor, V. Harris, E. Carpenter, J. Appl. Phys. 87 (2000) 6223–6228.
[6] M.R. DeGuide, R.C. O'Handley, G. Kalonji, J. Appl. Phys. 65 (1989) 3167–3172.
[7] Proceedings of International Symposium on Metastable, Mechanically Alloyed and Nanocrystalline Materials, J. Metastable Nanocrystal. Mater. 13 (2001).
[8] V.V. Boldyrev, Russ. Chem. Rev. 75 (2006) 177–189.
[9] C. Suryanarayana, Mechanical Alloying and Milling, Marcel Dekker, Inc., New York, 2004.
[10] C. Suryanarayana, E. Ivanov, Mechanical alloying for advanced materials, in: F.D.S. Marquis (Ed.), Powder Materials: Current Research and Industrial Practices III, TMS, Warrendale, PA, 2003, pp. 169–178.
[11] H.J. Fecht, Nanostruct. Mater. 6 (1995) 33–42.
[12] M.H. Mahmoud, H.H. Hamdeh, J.C. Ho, M.J. O'Shea, J.C. Walker, J. Magn. Magn. Mater. 220 (2000) 139–146.
[13] V. Šepelák, D. Baabe, F.J. Litterst, K.D. Becker, J. Appl. Phys. 88 (2000) 5884–5893.
[14] V. Šepelák, M. Menzel, I. Bergmann, M. Wiebcke, F. Krumeich, K.D. Becker, J. Magn. Magn. Mater. 272–276 (2004) 1616–1618.
[15] C.N. Chinnasamy, A. Narayanasamy, N. Ponpandian, K. Chattopadhyay, Mater. Sci. Eng. A 304–306 (2001) 983–987.
[16] E. Manova, B. Kunev, D. Paneva, I. Mitov, L. Petrov, C. Estournès, C. d'Orléans, J.L. Rehspringer, M. Kurmoo, Chem. Mater. 16 (2004) 5689–5696.
[17] E. Manova, C. Estournès, D. Paneva, J.-L. Rehspringer, T. Tsoncheva, B. Kunev, I. Mitov, Hyperfine Interact. 165 (2005) 215–220.
[18] K.P. Chae, Y.B. Lee, J.G. Lee, S.H. Lee, J. Magn. Magn. Mater. 220 (2000) 59–64.
[19] M. Rajendran, R.C. Pullar, A.K. Bhattacharya, D. Das, S.N. Chintalapudi, C.K. Majumdar, J. Magn. Magn. Mater. 232 (2001) 71–83.
[20] A.M. Abdeen, O.M. Hemeda, E.E. Assem, M.M. El-Sehly, J. Magn. Magn. Mater. 238 (2002) 75–83.
[21] G. Caruntu, A. Newell, D. Caruntu, C.J. O'Connor, J. Alloys Compd. 434–435 (2007) 637–640.
[22] W.S. Chiu, S. Radiman, R. Abd-Shukor, M.H. Abdullah, P.S. Khiew, J. Alloys Compd. 459 (2008) 291–297.
[23] G. Baldi, D. Bonacchi, C. Innocenti, G. Lorenzi, C. Sangregorio, J. Magn. Magn. Mater. 311 (2007) 10–16.
[24] P.C.R. Varma, R.S. Manna, D. Banerjee, M.R. Varma, K.G. Suresh, A.K. Nigam, J. Alloys Compd. 453 (2008) 298–303.
[25] A.T. Ngo, M.-P. Pileni, Adv. Mater. 12 (2000) 276–279.
[26] C. Estournès, C. D'Orléans, J.-L. Rehspringer, E. Manova, B. Kunev, D. Paneva, I. Mitov, L. Petrov, M. Kurmoo, Hyperfine Interact. 165 (2005) 61–67.
[27] G.K. Williamson, W.H. Hall, Acta Metall. 1 (1953) 22–31.
[28] G. Busca, V. Lorenzelli, V. Escribano, Chem. Mater. 4 (1992) 595–605.
[29] R.D. Waldron, Phys. Rev. 99 (1955) 1727–1735.
[30] J.B. Silva, W. Brito, N.D.S. Mohallem, Mater. Sci. Eng. B 112 (2004) 182–187.
[31] B. Lefez, P. Nkeng, J. Lopitaux, G. Poillerat, Mater. Res. Bull. 31 (1996) 1263–1267.
[32] G.A. Sawatzky, F. Van der Woude, A.H. Morrish, J. Appl. Phys. 39 (1968) 1024–1206.
[33] G.A. Sawatzky, F. Van der Woude, A.H. Morrish, Phys. Rev. 187 (1969) 747–757.
[34] P.M.A. de Bakker, R.E. Vandenberghe, E. de Grave, Hyperfine Interact. 94 (1994) 2023–2027.
[35] Y. Ahn, E.J. Choi, S. Kim, H.N. Ok, Mater. Lett. 50 (2001) 47–52.
[36] C. Estournès, T. Lutz, J. Happich, T. Quaranta, P. Wissler, J.L. Guille, J. Magn. Magn. Mater. 173 (1997) 83–92.
[37] M. Grigorova, H.J. Blythe, V. Blaskov, V. Rusanov, V. Petkov, V. Masheva, D. Nihtianova, M. Martinez, J.S. Munõz, M. Mikhov, J. Magn. Magn. Mater. 183 (1998) 163–172.
[38] C.N. Chinnasamy, B. Jeyadevan, K. Shioda, K. Tohji, D.J. Djayaprawira, M. Takahashi, R.J. Joseyphus, A. Narayanasamy, Appl. Phys. Lett. 83 (2003) 2862–2864.
[39] L.D. Tung, V. Kolesnichenko, D. Caruntu, N.H. Chou, C.J. O'Connor, L. Spinu, J. Appl. Phys. 93 (2003) 7486–7488.
[40] V. Kumar, A. Rana, M.S. Yadav, R.P. Pant, J. Magn. Magn. Mater. 320 (2008) 1729–1734.